
Development of a reduced-order model for wind turbine response to atmospheric turbulence in forest regions

Nebenführ, Bastian^{1,2,4†*)}, Carlen, Ingemar³⁾, Caracoglia, Luca⁴⁾, Davidson, Lars^{1,2)}

1) *Dept. of Applied Mechanics, Chalmers University of Technology, Gothenburg, Sweden*

2) *Swedish Wind Power Technology Center (SWPTC), Sweden*

3) *Teknikgruppen AB, Stockholm, Sweden*

4) *Dept. of Civil and Environmental Engineering, Northeastern University, Boston, MA, USA*

†) *Visiting Research Assistant, Northeastern University, April – July 2013*

*) *presenting author, basneb@chalmers.se*

ABSTRACT

A reduced-order structural model of a wind turbine has been developed and coupled with wind shear and turbulence fields generated computationally by Large-Eddy Simulation (LES). The wind turbine is composed of rigid but rotating blades on top of a flexible tower structure. Turbulence data from LES over a forest and over low-roughness flat terrain were tested in the proposed model. It was found that, while maintaining the same mean wind speed at the hub height, turbulence appears strongly increased in the atmospheric boundary layer above a forest. Subsequently, the dynamic loads on the wind turbine structure are more than doubled for the case with forest.

1 INTRODUCTION

Wind turbines are more often placed in forested regions nowadays. Above a forest, however, the atmospheric boundary layer is characterized by fairly low wind speeds with strong wind shear and strong turbulence right above the canopy. The turbulence leads to large fluctuating aerodynamic loads on the entire wind turbine structure and the wind shear induces strong cyclic loading on the rotating wind turbine blades. Since wind turbines are usually not designed for forest conditions, the encountered loads will shorten both the maintenance interval and the fatigue lifetime of the wind turbine components. There are indications that the design criteria are exceeded quite frequently in forest conditions (Bergström et al., 2013). In order to make an estimation of the aerodynamic loads of a wind turbine in a forest region, time-dependent turbulent flow fields need to be available. In this work, Large-Eddy Simulation (LES) is used for determining the flow field above a forest. For the sake of comparison, a LES without the forest is also included. Recent studies (Sim, et al., 2012, Lee, et al., 2012, Park, et al., 2013), in which LES turbulence fields were used as input for load calculations with the FAST code, have shown the feasibility of the chosen approach. Expectations are that there will be increased turbulence and increased wind shear in the case with the forest and hence increased aerodynamic loads on the wind turbine.

To be able to estimate the wind turbine loads in a fast and easy manner, a reduced-order structural model of a wind turbine has been developed. The model is then coupled with wind shear and turbulence fields over a forest, computationally generated by LES (Nebenführ & Davidson, 2013); the model is employed to analyze fluid-structure interaction effects on a standard wind turbine. Some of the results, obtained with the proposed model, are compared to results from the well-established structural analysis program *ViDyn* (Ganander & Olsson, 1998, Ganander, 2003).

2 MODEL DESCRIPTION

In the model, the wind turbine blades are represented as rigid elements, rotating about the horizontal axis of the rotor, and placed at the top of a flexible tower. The mass of each blade is concentrated, for simplicity, at the tip of the rigid element. Contributions of the nacelle and hub are exclusively taken into account in terms of additional mass and inertia terms at the top of the tower. The equations of motion for the flexible tower structure read:

$$\mathbf{M}\ddot{\underline{x}} + \mathbf{C}\dot{\underline{x}} + \mathbf{K}\underline{x} = \underline{f} \quad (1)$$

where bold capital letters denote matrices, under-bars denote vectors and the “dot” symbol designates derivation with respect to time. The effect of the rotor blades on the wind turbine tower is taken into account as both a concentrated force and a bending moment at the top of the tower. They are added as external forces in the force vector \underline{f} on the right-hand side of Eq. (1). An unsteady Blade-Element Momentum (BEM) method (Hansen, 2008) is used to calculate the rotor force and moment based on the instantaneous value of turbulent wind velocity, variable along each blade, supplied from the LES simulations and accounting for the fluid-structure effect induced by the vibrating tower. The tower is simulated by discretization of the structure into beam elements with lumped masses at discrete nodes along the height of the structure. A total of 15 nodes are used in the model. In Eq. (1) for the sake of simplicity, only the fore-aft deflection and a rotation around the lateral axis are considered in the dynamic response vector (\underline{x}) (i.e., response in the plane of the mean wind direction). This means that every node in the tower has two degrees-of-freedom (DOF). The NREL 5MW reference wind turbine in its on-shore configuration has been chosen for validation of the model. A full description of this wind turbine, including all structural information, is given by Jonkman et al., (2009). Equation (1) is subsequently reduced to state-space formulation and then solved numerically using a 4th order Runge-Kutta-Fehlberg (RKF) algorithm (Sewell, 2005) with varying time-step size. Numerical convergence is estimated as the difference between the 4th and a 5th order RKF solution. Since only fore-aft DOFs are taken into account in this model, yaw misalignment was disregarded. This means that the velocity field is normal to the rotor plane at every instant. In the following, we will refer to the above model as the reduced-order model (ROM).

Discretizing the tower into 15 equidistantly spaced elements yields the first three natural fore-aft bending frequencies given in Table 1. For comparison, the first and second fore-aft frequencies of the tower obtained by FAST and ADAMS (Jonkman, Butterfield, Musial, & Scott, 2009) are also given in Table 1; frequencies are obtained when the turbine is in the “parked” condition. The ROM determines somewhat higher natural frequencies than the FAST and ADAMS codes, but they are in the same range. This result indicates that the geometry and dynamical properties of the wind turbine are represented correctly in the model. A constant modal damping ratio equal to 1% with respect to critical is assumed in the simulations for all eigenmodes.

Table 1: Natural frequencies of the tower in (Hz)

Natural frequency	ROM	FAST	ADAMS
λ_1	0.3353	0.3240	0.3195
λ_2	2.9439	2.9003	2.8590
λ_3	7.8524	N/A	N/A

3 RESULTS

3.1 Large-Eddy Simulations

Large-Eddy Simulation solves the time-dependent, three-dimensional, filtered Navier-Stokes equations. Large turbulent scales that are above a certain filter size (usually the grid size) are resolved (calculated explicitly), while scales smaller than the grid size are parameterized using a so-called Sub-Grid Scale (SGS) model. As a large part of the turbulence spectrum is resolved, turbulence data from LES is considered to be more physically relevant than turbulence generated by statistical means. Additionally to the atmospheric turbulence, data from LES inherently contains information about wind shear and wind veer as well. This makes LES a powerful tool for generating turbulent inflow wind fields for the use in wind turbine load calculations. In the present study, two LES have been carried out for the atmospheric boundary layer. In one of the cases, a forest has been included in the computations, while in the other case a low-roughness flat terrain with a surface roughness of $z_0 = 0.02$ m was simulated. The latter case can be regarded as being representative of a grass-covered open landscape (Wieringa, 1992).

The simulations were carried out in a rectangular computational domain with the dimensions $(x,y,z) = (4H,2H,H)$, where x , y and z denote the streamwise, lateral and vertical directions, respectively. The domain height H was set to 400 m and a grid of $(n_x, n_y, n_z) = (192, 96, 96)$ cells was used for discretization of the domain. In the horizontal directions, the grid spacing was kept constant, while the grid was geometrically stretched by 8.5% in vertical direction above a height of 170 m (above the swept rotor area). Sampling the wind field at each cell in vertical and every second cell in horizontal direction, yields a constant grid over the swept rotor area with a resolution of 8x5 m for the load calculations. The data was sampled at each computational time step. The time step size in the LES is set to $\Delta t = 0.1$ s, which ensures a CFL number of less than 0.5 in the entire domain. A horizontally homogeneous forest with a height of $h = 20$ m is included in the lowest part of the domain, where the forest is represented in terms of a drag force (Shaw & Schumann, 1992). The low-roughness case was simulated on the same computational grid, simply by deactivating the drag force.

Figure 1 displays the horizontal wind speed profile and the vertical momentum flux obtained for the LES with forest. Both quantities are normalized with the friction velocity, u^* , calculated at $z = 2h$, in order to compare them with field measurements. The friction velocity is defined in Eq. (2).

$$u^* = \left(\overline{u'w'^2} + \overline{v'w'^2} \right)^{1/4} \quad (2)$$

Good agreement with the measurements is achieved both in terms of velocity and flux profiles. This gives confidence in the numerical results. In order to provide comparable input for the load calculations, the wind fields of the two simulations have been scaled to a mean wind speed at hub-height of $V_{hub} = 8$ m/s. The scaled profiles of the two LES are shown in Figure 2 (a). Also a fit of the wind profile following the power-law function, $V(z) = V_r (z/z_r)^\alpha$, is included. The exponent, α , is set to 0.4 and 0.15 for the with- and without-forest case, respectively. It becomes clear that the wind shear in the forest case exceeds the suggested design criterion of the IEC, which is given as $\alpha = 0.2$ (IEC, 2005). The power spectral density (PSD) plot of the fluctuating wind speed at hub-height is depicted in Figure 2 (b). One can observe that the case including the forest contains more energy-bearing large-scale fluctuations (low frequencies), while the absence of a forest leads to slightly higher small-scale turbulence. In general, the inertial sub-range of the energy spectrum is well predicted in both cases, with a clearly visible -5/3 decay for more than one decade. The highest resolved frequency is limited by the ratio of the grid resolution and the standard deviation of the velocity fluctuation. Since the same grid is used in both cases and the velocity fluctuations are smaller in the low-roughness case, the cut-off frequency is slightly higher in that case.

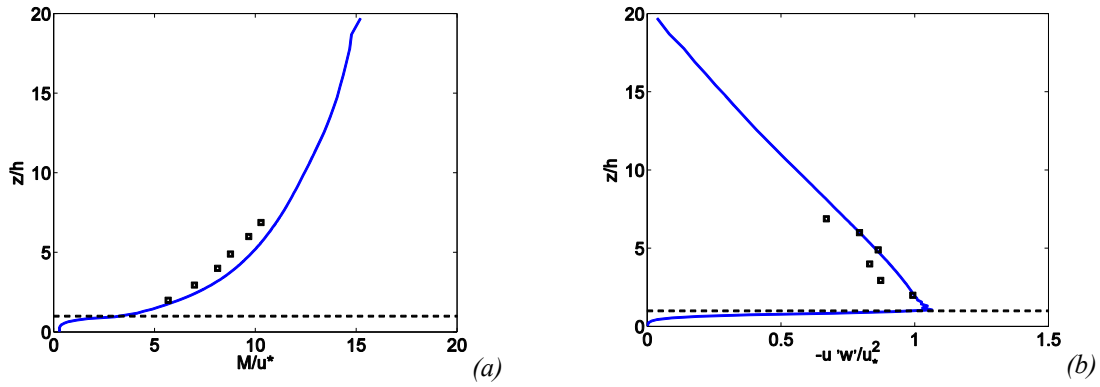


Figure 1: Validation of numerical simulations (forest case); —: LES, \square : measurement, ---: canopy top, (a) horizontal wind speed, (b) vertical momentum flux

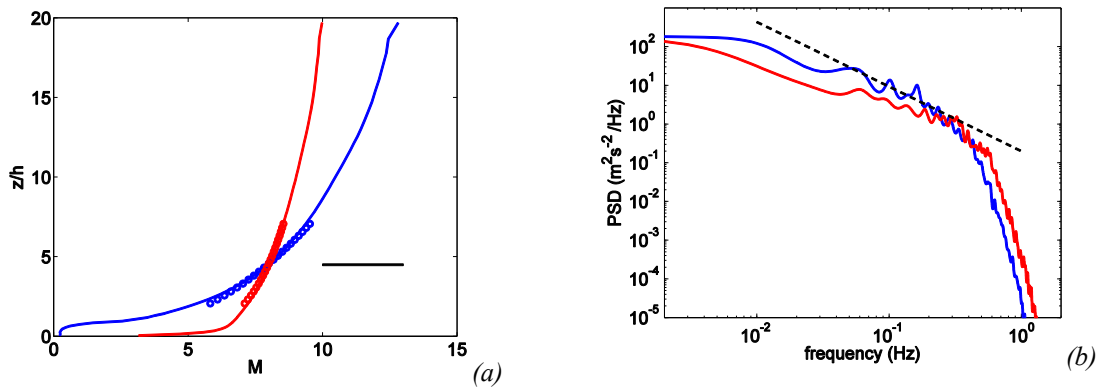


Figure 2: Comparison of the two LES cases. —: with forest, —: without forest, —: hub-height ($z/h=4.5$), ---: -5/3 slope, \circ : $\alpha=0.4$, \circ : $\alpha=0.15$ (a) horizontal wind speed, (b) PSD of velocity fluctuations at hubheight

3.2 Load calculations with the ROM

The ROM does not include a control system and hence, the considered case is calculated with a constant blade-pitch angle of $\theta_{pitch}=0^\circ$ and a constant rotational speed of $\Omega=12.1$ rpm.

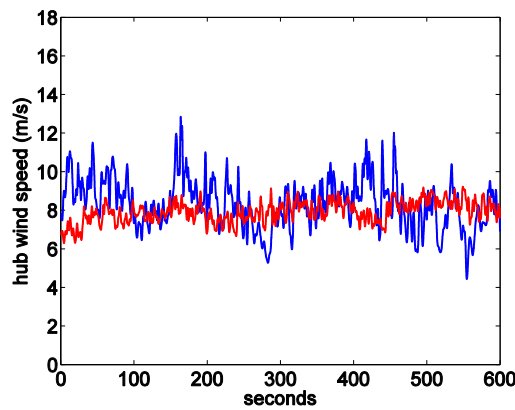


Figure 3: Hub-height wind speed for the two cases; —: with forest, —: without forest

Table 2 gives an overview over the mean value and the root mean square (RMS) of the wind speed at hub height. It can be seen that, as a result of scaling, the mean wind speed is similar in both cases. One initial expectation was that the forest would induce stronger turbulence, which is confirmed by the numerical simulations. The simulations suggest a considerable increase in turbulence intensity by more than a factor two for the case with forest. Similar results have been presented by Chougule et al. (2014) for field measurements. As the turbulent input to the reduced-order model considerably differs between the two LES, much larger loads are expected to be seen for the with-forest case.

Table 2: Hub-height wind speed, mean and RMS in (m/s).

Case	Hub-height wind speed	
	Mean	RMS
Forest	8.18	1.33
No forest	7.91	0.55

In Figure 4 (a), the horizontal displacement of the wind turbine nacelle, in the direction of the mean wind, is presented. The data covers only the stationary response, i.e. the initial transient of the wind turbine response has been neglected. Comparable mean deflections of about 0.27 m for the with-forest case and 0.25 m for the without-forest case are found as a result of the similar mean wind speeds at hub level in the two cases. The response in the with-forest case shows significantly larger fluctuations and thus the standard deviation is about twice that of the case without forest. This is not surprising considering the large difference in standard deviation of the turbulent input. Translating the time-history of the nacelle deflection into frequency domain yields the PSD plot of Figure 4 (b). It can be clearly seen that the case without forest contains significantly less energy, especially at low frequencies. This is a direct consequence of the turbulent kinetic energy contained in the wind field (compare Figure 2 (b)). Peaks are evident in the PSD of both cases for the natural frequencies of the wind turbine tower (λ_1 , λ_2 , λ_3) and the rotational frequency of the rotor (1P). The forest case shows additional peaks for multiples of the rotational frequency (3P, 6P). Further peaks appear in the PSD for frequencies above 10Hz; these correspond to higher modes of the wind-turbine tower structure.

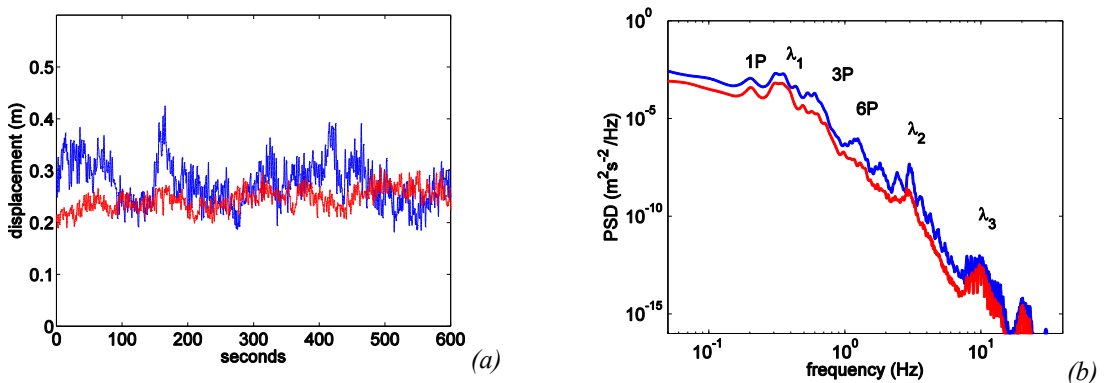


Figure 4: Nacelle displacement, —: with forest, —: without forest.
(a) time-history, (b) PSD

For comparison, load calculations have also been performed using the structural analysis program *ViDyn*. In Figure 5, the time-histories of the tower base bending moment (TBBM) obtained by the ROM and *ViDyn* are presented. The trends and mean values are in good agreement for both

models. However, the ROM yields a more rapidly fluctuating result. It is believed that this is a consequence of using rigid blades. In this case, variations in the wind field provoke an immediate response of the wind turbine. On the contrary, the flexible blades used in *ViDyn* along with inertia in the generator, will prevent an immediate response and the small scale fluctuations are “filtered out”. Moreover, in the case of a rigid blade the energy originating from the dynamic load is transferred to the tower entirely (as kinetic energy), which later becomes elastic energy. When vibration in the blades is allowed, elastic energy is redistributed among all components, leading to a lower tower response at higher modes. Hence, the higher natural frequencies of the tower are not excited in *ViDyn*. That is why the ROM yields a higher number of effective cycles and subsequently an increased equivalent fatigue load (EFL) as indicated in Table 3. The EFL is calculated according to Eq. (3).

$$EFL = \sqrt[m]{\sum_{i=1}^N \frac{S_i^m}{N_0}} \quad (3)$$

Where N is the number of effective cycles, S_i are the load amplitudes, $m=3$ is the Woehler exponent for the steel tower and $N_0=1000$ is used for normalization. In this case, the EFL gives the fatigue load that would be caused by N_0 cycles with constant load amplitude. A good review of the calculation of equivalent fatigue loads is given by Ragan and Manuel (2007). While the *ViDyn* result indicates an increase in EFL of about 60% for the forest case, the ROM yields an increase of about 13%. It is furthermore evident from **Figure 5: Tower base bending moment**; **—: with forest**, **—: without forest**,

(a) ROM, **(b) ViDyn** Figure 5 that the TBBM for the forest case is strongly increased compared with the low-roughness terrain.

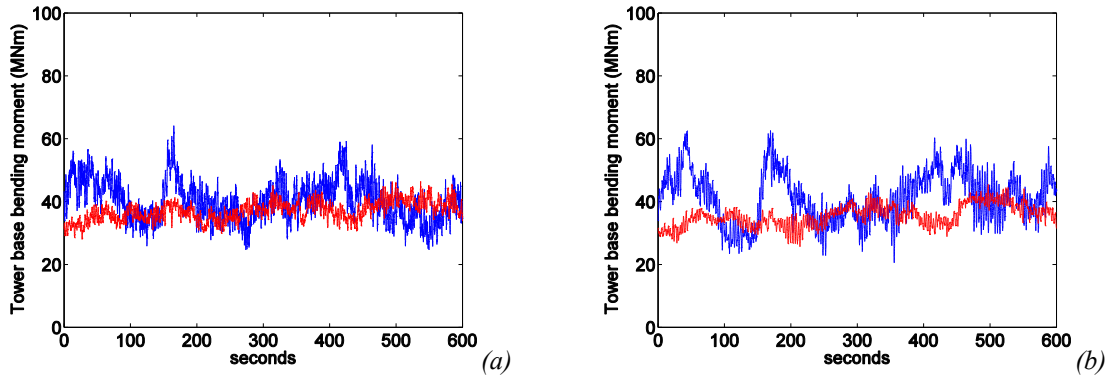


Figure 5: Tower base bending moment; —: with forest, —: without forest, (a) ROM, (b) ViDyn

Figure 6 displays a comparison of the fatigue load histograms, generated through rain-flow counting (ASTM, 2005), for the ROM and *ViDyn*. As already mentioned, a larger number of effective cycles is obtained with the ROM result. Nevertheless, the trends towards higher loads for the forest case are evident and also suggested by both models.

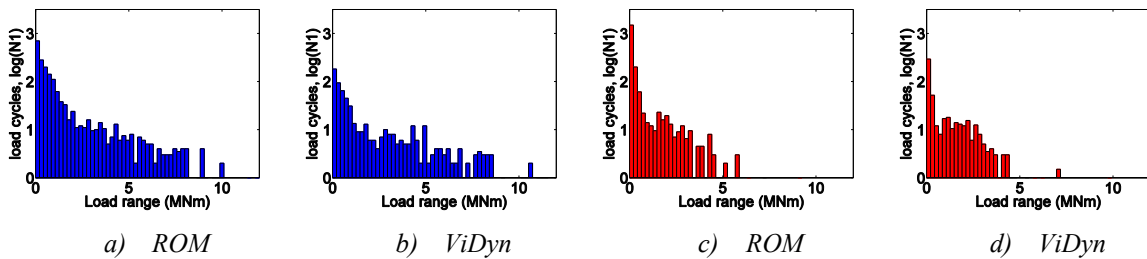


Figure 6: Fatigue load histograms of the tower base bending moment.
(a), (b) with forest, (c), (d) without forest

It should be noted that in this study, the rain-flow counting method was only applied to the internal bending moment at the base of the structure. Internal stress cycles for fatigue in other components or connection elements were not investigated, but could readily be considered for future simulations. Moreover, the presented results are based on one realization of the wind field and dynamic system response. A more detailed probabilistic analysis would be required to account for the variability in the internal forces and stresses. This is, however, beyond the scope of this study.

Table 3: Tower base bending moment, mean, RMS and EFL values in (MNm),
 N =effective number of cycles

Case	ROM				ViDyn			
	Mean	RMS	N	EFL	Mean	RMS	N	EFL
Forest	40.3957	6.3225	1826	18.6500	41.3440	7.9608	623	9.2990
No forest	36.9924	3.0810	1959	16.4632	35.5205	3.4250	520	5.8057

4 CONCLUSIONS

A reduced-order structural model of the NREL 5MW reference wind turbine was presented. In the model, rigid but rotating blades are placed on top of a flexible tower. Turbulent wind field data, sampled from Large-Eddy Simulations, has been used for testing the proposed model. One of the LES represents the flow over a horizontally homogeneous forest, while the other represents flow over a low-roughness flat terrain. The simulations suggest that turbulent fluctuations in the with-forest case might be two times larger compared to the case without forest. Moreover, it is shown that the wind shear in the forest case greatly exceeds the IEC design criterion. The proposed model yields largely increased fluctuating loads for the forest case. The standard deviation of the tower base bending moment is predicted to be roughly doubled by the presence of the forest environment. Rain-flow counting of the tower base bending moment time-history resulted in higher equivalent fatigue loads and an increased number of effective cycles for the reduced-order model compared to *ViDyn*. This is believed to be an effect of the rigid blades, which allow for an “immediate transfer” of the loads from the fluctuating wind field. However, the ROM is able to give an acceptable estimation of the expected loads on wind turbines for various wind and loading conditions.

Acknowledgements

The authors are thankful to Johan Arnquist (Uppsala University), Ebba Dellwik (DTU) and Hans Bergström (Uppsala University) for providing the field measurement data. The data was gathered in the framework of the Swedish Vindforsk project. This project is financed through the Swedish Wind Power Technology Center (SWPTC). SWPTC is a research center for design of wind turbines. The purpose of the center is to support Swedish industry with knowledge of design techniques as well as maintenance in the field of wind power. The center is funded by the Swedish Energy Agency, Chalmers University of Technology as well as academic and industrial partners. This work was initiated during the first author’s study and research period at Northeastern University, Boston, Massachusetts, USA in 2013.

References

- ASTM. (2005). *ASTME, 1049-85: Standard practices for cycle counting in fatigue analysis*. ASTM International.
- Bergström, e. a. (2013). *Wind Power in Forests - Winds and effects on loads*. Stockholm.
- Chougule, A., Mann, J., Segalini, A., & Dellwik, E. (2014). Spectral tensor parameters for wind turbine load modeling from forested and agricultural landscapes. *Wind Energy*. doi:10.1002/we.1709
- Ganander, H. (2003). The Use of a Code-Generating System for the Derivation of the Equations for Wind Turbine Dynamics. *Wind Energy*, 6(4), 333-345.
- Ganander, H., & Olsson, B. (1998). *ViDyn: Simulation program for horizontal axis windpower plants*. Stockholm, Sweden: Teknikgruppen AB.
- Hansen, M. (2008). *Aerodynamics of wind turbines* (2nd ed.). London: Earthscan.
- IEC. (2005). *IEC 61400-1 Wind Turbines Part1: Design Requirements*. Geneva: International Electrotechnical Commission.
- Jonkman, J., Butterfield, S., Musial, W., & Scott, G. (2009). *Definition of a 5-MW reference wind turbine for offshore system development*. Colorado, USA: National Renewable Energy Laboratory (NREL).
- Lee, S., Churchfield, M., Moriarty, P., Jonkman, J., & Michalakes, J. (2012). Atmospheric and Wake Turbulence Impacts on Wind Turbine Fatigue Loadings. Proceedings of 50th AIAA Aerospace Sciences Meeting: Nashville, TN.
- Nebenführ, B., & Davidson, L. (2013). Large-Eddy Simulation for Wind Turbine Fatigue Load Calculation in Forest Regions. *Proceedings of 9th PhD Seminar on Wind Energy in Europe, September 18-20, 2013*. Proceedings of the 9th PhD Seminar on Wind Energy in Europe: Uppsala University Campus Gotland, Sweden.
- Park, J., Basu, S., & Manuel, L. (2013). Large-eddy simulation of stable boundary layer turbulence and estimation of associated wind turbine loads. *Wind Energy*.
- Ragan, P., & Manuel, L. (2007). Comparing estimates of wind turbine fatigue loads using time-domain and spectral methods. *Wind Engineering*, 83-99.
- Sewell, G. (2005). *The numerical solution of ordinary and partial differential equations* (2nd ed.). Hoboken, New Jersey, USA: John Wiley and Sons.
- Shaw, R., & Schumann, U. (1992). Large-Eddy Simulation of Turbulent Flow above and within a Canopy. *Boundary-Layer Meteorology*, 47-64.
- Sim, C., Basu, S., & Manuel, L. (2012). On Space-Time Resolution of Inflow Representations for Wind Turbine Loads Analysis. *Energies*, 5(7), 2071 - 2092.
- Wieringa, J. (1992). Updating the Davenport roughness classification. *Journal of Wind Engineering and Industrial Aerodynamics*, 357-368.
-